Evaluation of Homology Modeling of G-Protein-Coupled Receptors in Light of the A_{2A} Adenosine Receptor Crystallographic Structure

Andrei A. Ivanov,[†] Dov Barak,[‡] and Kenneth A. Jacobson*[,†]

Molecular Recognition Section, Laboratory of Bioorganic Chemistry, National Institute of Diabetes and Digestive and Kidney Diseases, National Institutes of Health, Bethesda, Maryland 20892, and Israel Institute for Biological Research, Ness Ziona, Israel

Received December 4, 2008

Homology modeling of the human A_{2A} adenosine receptor (AR) based on bovine rhodopsin predicted a protein structure that was very similar to the recently determined crystallographic structure. The discrepancy between the experimentally observed orientation of the antagonist and those obtained by previous antagonist docking is related to the loop structure of rhodopsin being carried over to the model of the A_{2A} AR and was rectified when the β_2-adrenergic receptor was used as a template for homology modeling. Docking of the triazolotriazine antagonist ligand ZM241385 **1** was greatly improved by including water molecules of the X-ray structure or by using a constraint from mutagenesis. Automatic agonists docking to both a new homology modeled receptor and the A_{2A} AR crystallographic structure produced similar results. Heterocyclic nitrogen atoms closely corresponded when the docked adenine moiety of agonists and **1** were overlaid. The cumulative mutagenesis data, which support the proposed mode of agonist docking, can be reexamined in light of the crystallographic structure. Thus, homology modeling of GPCRs remains a useful technique in probing the structure of the protein and predicting modes of ligand docking.

Introduction

Crystallographic structural data are available today for four different GPCRs: bovine rhodopsin,[1] human β_2-adrenergic receptor,[2] turkey β_1-adrenergic receptor,[3] and human A_{2A} adenosine receptor (AR^a).[4] All of these receptors are transmembrane proteins consisting of seven α-helices connected by three extracellular (ELs) and three intracellular loops (ILs). The general configuration of the transmembrane domains (TMs) is very similar for all GPCRs. In particular, the heavy atoms of TMs of the A_{2A} AR and β_2AR can be superimposed with a rmsd of 1.90Å, and the superimposition of α-helices of the A_{2A} AR and rhodopsin provided a rmsd value of 2.16 Å. The differences in the configuration of TMs of rhodpsin and the β_2AR are represented by a rmsd of 1.90 Å.

Since for a long time the only GPCR for which an experimental structure was available was bovine rhodopsin, rhodopsin was widely used as a template for homology modeling of other GPCRs. One of the first molecular models constructed for GPCRs was a model of the human A_{2A} AR based on the low resolution electron density map of rhodopsin.[5] During recent years, numerous homology models have been generated for various GPCRs, including the A_{2A} and other subtypes of ARs.[6−8] Many of the models proposed were successfully used for investigation of ligand−receptor interactions and the development of novel biologically active compounds, in particular, for the ARs.[9] Now with an experimental structure of the A_{2A} AR available it is possible to evaluate the quality of the proposed models and to refine hypotheses concerning the ligand binding modes. With this aim we compared our previously published rhodpsin-based model of the A_{2A} AR[6] (PDB code 1UPE) with the X-ray structure of this receptor.

Chart 1. Structure of representative antagonist (**1**, **2**) and agonist (**3**, **4**) AR ligands

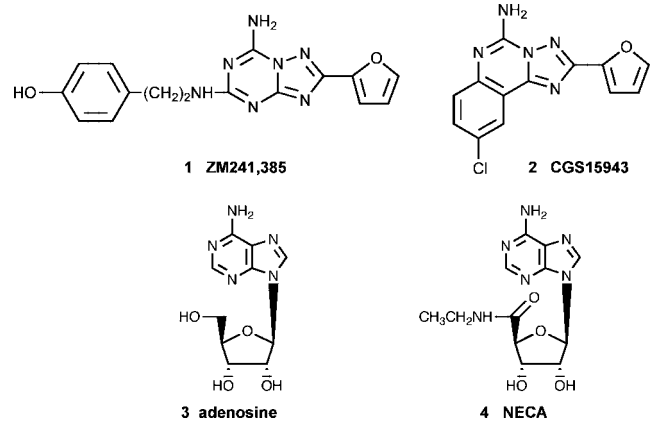

The docking orientation of the antagonist ligand 4-2-[7-amino-2-(2-furyl)-1,2,4-triazolo[1,5-a][1,3,5]triazin-5-yl-amino]ethylphenol **1** (ZM241385)[10] (Chart 1) in the human A_{2A} AR was different from the antagonist docking modes typically predicted previously by modeling. A predicted antagonist binding site, e.g., for *N*-[9-chloro-2-(2-furanyl)[1,2,4]triazolo[1,5-c]quinazolin-5-amine **2** (CGS15943),[6] corresponded more closely to the position of the retinal binding site in rhodopsin and the binding site of the inverse agonist carazolol in the β_2-adrenergic receptor. In this study we have evaluated the use of molecular modeling of GPCRs and ligand docking in light of the newly reported crystallographic structures of the A_{2A} AR and other GPCRs. Costanzi studied the β_2-adrenergic receptor structure and its docked ligand to conclude that

* To whom correspondence should be addressed. Address: Molecular Recognition Section, Building 8A, Room B1A-19, NIH, NIDDK, LBC, Bethesda, MD 20892-0810. Phone: (301) 496-9024. Fax: (301) 480-8422. E-mail: kajacobs@helix.nih.gov.

† National Institute of Diabetes and Digestive and Kidney Diseases.

‡ Israel Institute for Biological Research.

[a] Abbreviations: AR, adenosine receptor; β_2AR, β2-adrenergic receptor, EL, extracellular loop; GPCR, G-protein-coupled receptor; NECA, 5′-*N*-ethylcarboxamidoadenosine; rmsd, root mean squared deviation; TM, transmembrane helical domain.

10.1021/jm801533x CCC: $40.75
Published on Web 04/29/2009

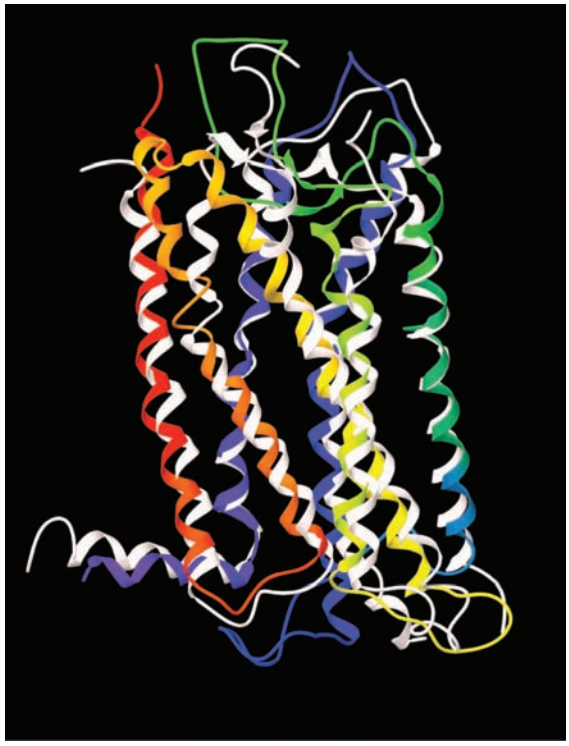

Figure 1. Superimposition of the crystal structure of the human A_{2A} AR (white) with the structure of the human A_{2A} AR predicted with molecular modeling (1UPE). All atoms of amino acid residues located in TMs were superimposed with a rmsd of 2.37 Å.

GPCR modeling is applicable to the design of site-directed mutagenesis experiments and to drug discovery.[11] We have extended the analysis to the adenosine system.

Results

Comparison of the A_{2A} AR Structures: Predicted Homology Model vs Crystallographic Structure. All atoms of the α-helical TMs of a previously published rhodopsin-based homology model of the A_{2A} AR[6] and the X-ray structure of this receptor were aligned with a rmsd value for all TM atoms of 2.37 Å. Not surprisingly, the configuration and orientation of the TMs of the theoretical model and experimental structure of the A_{2A} AR were found to be very similar (Figure 1). In contrast, the configurations of the ELs are significantly different in these two structures.

Previously, various residues located mostly in TMs 3, 5, 6, and 7 were predicted with modeling to be involved in ligand recognition (Supporting Information, Table S1).[6,12,13] In particular, it was suggested that Ile80 (3.28), Val84 (3.32), Leu85 (3.33), Thr88 (3.36), Gln89 (3.37), Ile135 (4.56), Leu167 (EL2), Phe168 (EL2), Asn181 (5.42), Phe182 (5.43), Val186 (5.47), Trp246 (6.48), Leu249 (6.51), His250 (6.52), Asn253 (6.55), Ile274 (7.39), Ser277 (7.42), His278 (7.43) are located in proximity to antagonist **2** and involved in interactions with the ligand[6] (the numbers in parentheses correspond to the Ballesteros−Weinstein indexing system).[14] The importance of residues located in the above-mentioned TM regions and in EL2 was confirmed by site-directed mutagenesis data obtained not only for the A_{2A} AR (Table S1) but also for other ARs and diverse GPCRs.[15] In agreement with the results of molecular modeling and pharmacological studies, many of these critical residues are located in proximity to the antagonist ligand **1** in the recent crystallographic structure of the A_{2A} AR. Examples of residues in proximity to the bound **1** in the X-ray structure that were

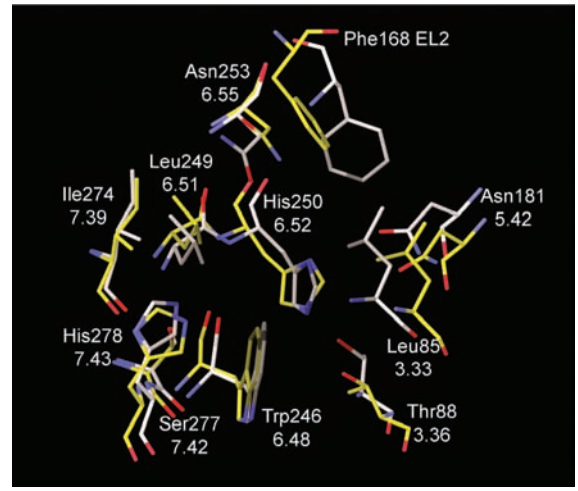

Figure 2. Superimposition of the critical amino acid residues of adenosine receptors. The carbon atoms of residues of the A_{2A} AR X-ray structure are shown in yellow, and the C-atoms of residues of the A_{2A} AR homology model (1UPE) are shown in white.

predicted by modeling to be involved in antagonist recognition are Leu85 (3.33), Phe168 (EL2), Asn181 (5.42), Trp246 (6.48), Leu249 (6.51), Asn253 (6.55), Ile274 (7.39) (Supporting Information, Table S1).[6] The differences in orientation of side chains of these amino acid residues between the homology model and X-ray structure were examined. It is noted that the antagonist bound X-ray structure of the A_{2A} AR was compared with the original rhodopsin-based model of the A_{2A} AR.[6] Since the inactive, retinal-bound structure of rhodopsin was used as a template for the modeling, the A_{2A} AR model is more related to the ground-state of the receptor and therefore can be compared with an antagonist occupied X-ray structure.

As shown in Figure 2, homology modeling demonstrated an excellent ability to predict the correct orientation of residue side chains. The residues in their predicted orientation fit very well to the experimental structure. In addition, it was found that superimposition of Cα-atoms of selected residues in the ligand binding pocket, i.e., Thr88 (3.36), Asn181 (5.42), Trp246 (6.48), His250 (6.52), Asn253 (6.55), Ser277 (7.42), His278 (7.43), Ile274 (7.39), provided an rmsd value of 0.90 Å. The proximity of the side chains of conserved His278 in TM7 and a Glu13 in TM1, previously identified through the combination of modeling and mutagenesis for both A_{2A} and A_3 ARs,[16,17] was confirmed in the X-ray structure. Also, the H-bonding between the backbone carbonyl group of Ser281 (7.46) and the side chain amino group of Asn24 (1.50) and a H-bonding between Ser281 (7.46) and Asp52 (2.50) side chains were previously predicted by the modeling. These interactions were observed in the recent A_{2A} AR crystal structure. In addition, the proximity of Asn24 (1.50) to Asp52 (2.50) was suggested on the basis of the modeling studies. In the A_{2A} AR crystal structure the side chains of these two residues appear to be connected through a water molecule. Thus, the comparison performed clearly demonstrated the ability of a homology modeling approach to provide an accurate model of a GPCR protein structure, especially within its TM domains.

Interestingly, several residues shown by mutagenesis to be critical for antagonist binding are not involved in direct contact with **1** in the recent A_{2A} AR crystal structure. Thus, the involvement might conceivably be through intervening amino acid residues or a conserved bound water molecule. In particular, it was demonstrated that replacement of Phe182 (5.43), Ser281(7.46), or Phe257 (5.59) with Ala resulted in loss of

agonist and antagonist radioligand binding.[5] However, the F182Y mutation resulted in only 2-fold decreased antagonist affinity. In the crystal structure Phe182 is involved in $\pi-\pi$ interactions with His250 (6.52) and may play a role in helix−helix packing, as was suggested by Kim and co-workers.[5] More importantly, His250 is directly involved in the interaction with ligands, and the replacement of Phe182 may result in the repositioning of the His residue. Ser281 (7.46) was shown to be critical for both agonist and antagonist binding.[5] As mentioned above, in the X-ray structure this residue is involved in interhelical interactions. Namely, Ser281 forms a H-bond with Asp52 (2.50), which is highly conserved among all GPCRs. In contrast, Phe257 does not form significant interactions with other residues in the crystal structure, and this residue is oriented outwardly from the binding cavity. Thus, the involvement of certain residues in ligand recognition in the A_{2A} AR is now shown to be indirect.

Molecular Docking of Antagonist 1 to the A_{2A} AR Crystal Structure. To investigate an ability of molecular docking to reproduce an experimentally observed ligand binding mode, **1** was redocked to the crystal structure of the A_{2A} AR. Initially the Glide XP software was utilized to automatically dock **1** to the rigid binding site of the A_{2A} AR without any constraints and without the presence of water molecules. The results obtained indicated that the orientation of the ligand inside the receptor was inverted along the long axis compared with the crystal structure (Figure 3A). The differences in the position and orientation of **1** docked to the crystal structure and its experimental position were characterized by an $rmsd_1$ value of 10.27 Å.

The binding mode of **1** obtained after molecular docking performed with the MOE software was in better agreement with the experimental binding mode (Figure 3B). However, because of the differences in the orientation of the phenylethylamine chain, the $rmsd_1$ value of 6.11 Å between predicted and experimental positions of **1** was relatively high.

Compound **1** was also docked to the crystal structure of the A_{2A} AR containing the three water molecules that coordinated with the ligand in the X-ray structure. The ligand binding mode obtained was in an excellent agreement with the experimental binding mode (Figure 3C), $rmsd_1 = 0.90$ Å. In practice, predicting the accurate position of water molecules inside a ligand binding site is a challenge, which would hinder the general application of this finding to other GPCR modeling.

However, we found that data from site-directed mutagenesis to establish extra constraints in the model can greatly improve the accuracy of prediction. In particular, it was shown that Asn6.55 is critical for ligand binding at all four subtypes of ARs. Also, this residue formed a H-bond with the exocyclic amino group of **1**. Molecular docking of **1** to the rigid A_{2A} AR performed with the H-bond interaction between Asn253 (6.55) and the exocyclic amino group of exocyclic amino group of **1** used as a constraint provided a reasonable overlay between predicted and experimental binding modes of **1** ($rmsd_1 = 2.09$ Å, Figure 3D). In order to study the role of flexibility of the receptor side chains in the docking studies, the InducedFit approach was also utilized to redock **1** to the crystal structure. The analysis of the binding mode of **1** obtained after InducedFit docking revealed that the core heterocycle of the ligand had the same position and orientation inside the receptor as appeared in the crystal structure.

In contrast, the predicted conformation of the flexible phenylethylamine chain of **1** was found to be different compared with the X-ray structure. In the crystal structure, the OH-group

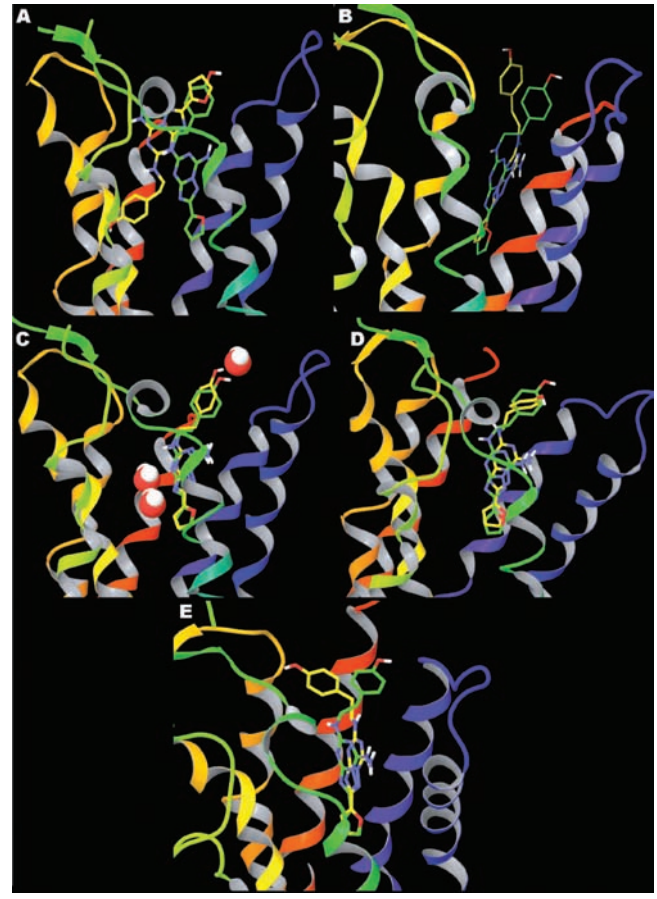

Figure 3. Results of molecular docking of **1** to the A_{2A} AR crystal structure: (A) Glide XP automatic docking to the rigid binding site performed without constraints and without the presence of water molecules, $rmsd_1 = 10.27$ Å; (B) results of molecular docking performed with the Tabu Search algorithm implemented in MOE software, $rmsd_1 = 6.11$ Å; (C) Glide XP automatic docking performed with the presence of three water molecules coordinated with **1** in the X-ray structure, $rmsd_1 = 0.90$ Å; (D) Glide XP molecular docking, where the H-bond between the exocyclic amino group of **1** and the side chain oxygen atom of Asn253 (6.55) was used as a constraint during the docking, $rmsd_1 = 2.09$ Å; (E) binding mode of **1** obtained after InducedFit docking, where the side chain oxygen atom of Asn253 (6.55) was used as the receptor H-bond constraint atom, $rmsd_1 = 3.58$ Å. The carbon atoms of **1** in the A_{2A} AR crystal structure are in green. The carbon atoms of **1** obtained after molecular docking are in yellow.

of the aryl ring is H-bonded with a water molecule. Since InducedFit docking was performed in the absence of water molecules, the interaction between the phenyl ring and water was obviously impossible. However, a H-bonded functional group is more favorable energetically than a noncoordinated functional group. For this reason, a H-bond between the OH-group of **1** and the backbone oxygen atom of Ile67 was formed during the InducedFit docking, resulting in a different conformation of the phenylethylamine chain. A $rmsd_1$ of 3.58 Å was found between the experimental position of **1** inside the A_{2A} AR and its position obtained after InducedFit docking (Figure 3E).

Binding Mode of Antagonists Docked in a Homology Modeled A_{2A} AR in Comparison to the Crystallographic Structure of Bound Compound 1. In the A_{2A} AR X-ray structure, the antagonist binding site was shifted closer to TMs 6 and 7 and closer to the exofacial side than the bound ligands carazolol and cyanopindolol in the previous adrenergic receptor structures.[2−4] Therefore, we examined the modeling of **1** binding in

greater detail. Several molecular models of the ARs with various antagonists docked have been proposed. Recently, a putative binding mode of **1** was examined with the molecular modeling approach by Yuzlenco et al.[23] However, most of the previous models concerned antagonists other than **1**. In most of the reported models, the amino acid residues predicted to be involved in antagonist recognition were in good agreement with the X-ray structure of the A_{2A} AR. For example, Kim and coworkers suggested an involvement of Leu85 (3.33), Phe168 (EL2), Asn253 (6.55), Ile274 (7.39) in the binding of the antagonist **2**.[6] In particular, the model proposed that Asn253 (6.55) was H-bonded to the exocyclic amino group of **2**, and Phe168 was found in proximity to its triazoloquinazoline core. Here, we modeled a complex of the A_{2A} AR, derived from a new homology model, with its antagonist **1** to compare the results of molecular modeling with the crystal structure.

First of all, a homology model of the A_{2A} AR to be utilized for studies of the docking of **1** was built on the basis of the recently reported crystal structure of the β_2AR. Since the configuration of EL2 is different in various GPCR crystal structures, an accurate prediction of the configuration of the entire loop was not attempted. However, the disulfide bridge formed between two conserved Cys residues located in TM3 and EL2 was observed in all available GPCR crystal structures. In view of this, in our model of the A_{2A} AR only part of EL2 (Cys166−Asn175) was constructed.

The obtained homology model was utilized for automatic docking of **1**, and the ligand binding mode obtained was found to be in good agreement with the experimental structure (Figure 7). In particular, in the resulting model Asn253 (6.55) formed a H-bond with the exocyclic amino group of **1**, and Phe168 was involved in $\pi-\pi$ interactions with the ligand triazolotriazine ring. The furanyl ring was oriented inside the receptor and was found in proximity to Leu85 (3.33), Thr88 (3.36), Trp246 (6.48), Leu249 (6.51). The 4-hydroxyphenylethylamine chain of **1** was oriented toward the extracellular region of the A_{2A} AR and was located between Ala265 (EL3) and Leu167 (EL2). Thus, the obtained binding mode of **1** corresponded very well to its binding mode observed in the crystal structure. This finding demonstrates the general applicability of the homology modeling approach to construct realistic models of GPCRs. The homology models of the A_{2A} AR based on rhodopsin and on the β_2AR are very similar in the region of the ligand binding pocket. Hence, the previous docking experiments, in which the ligands were not affected by the different loop structure, are expected to be valid.

Ligand Docking To Predict the Agonist Binding Mode. The published crystal structure of the A_{2A} AR with its antagonist **1** represents a conformation of the receptor resembling the inactive state. However, as in previous homology modeling studies based on the rhodopsin ground state, we assumed that this structure would be able to fit small agonists as well. With this assumption, the molecular docking of the principal native AR agonist, adenosine **3**, and the synthetic agonist 5′-*N*-ethylcarboxamidoadenosine (**4**, NECA) to the A_{2A} AR X-ray structure was performed automatically as described in Methods. It is noted that these computational studies were conducted using standard, automatic techniques implemented in currently favored and widely used software such as MOE and the Schrödinger package.[18,19] Standard procedures for protein refinement, such as the addition of missing hydrogens and the assignment of bond orders, were automatically performed during the protein preparation step. To take into account the flexibility of the receptor side chains, the InducedFit docking approach was utilized.[20]

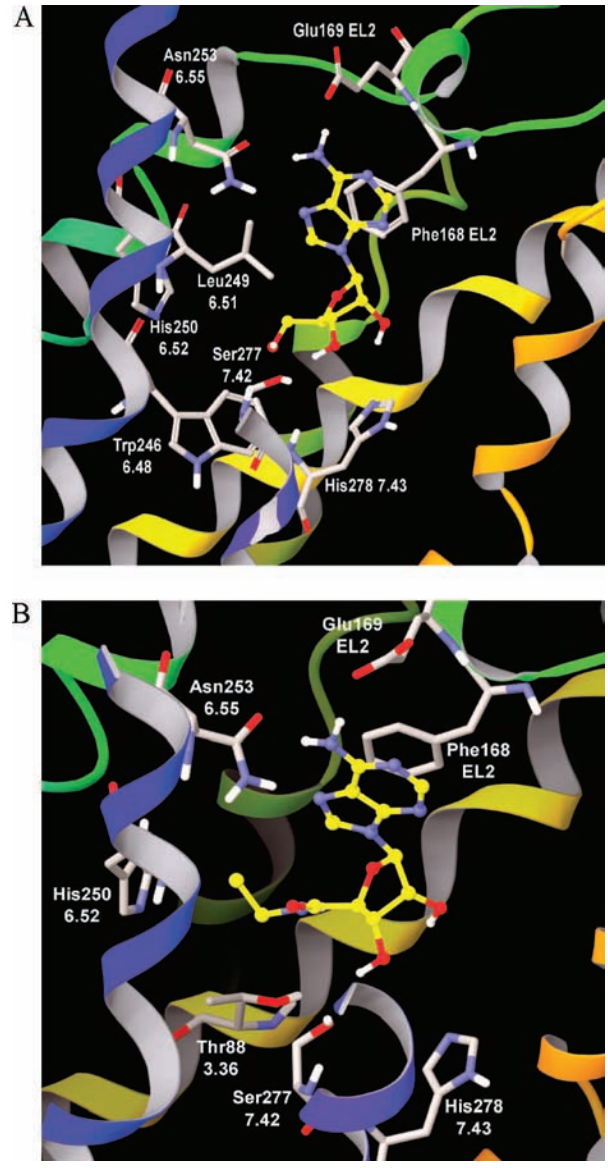

Figure 4. Binding mode of adenosine (A) and **4** (B) obtained after automatic docking to the crystal structure of A_{2A} AR.

The results of molecular docking revealed that both studied agonists fit well the X-ray structure of the A_{2A} AR and independently adopted very similar binding modes (Figure 4). In particular, the complexes obtained indicated that the N^6-amino group of the ligands could form a H-bond with Asn253 (6.55) and Glu169 (EL2). The adenine ring was involved in $\pi-\pi$ stacking with the aromatic ring of Phe168 (EL2), as was the heterocycle of **1** in the X-ray structure. The 2′- and 3′-OH groups were observed in proximity to Ser277 (7.42) and His728 (7.43) and can be involved in H-bonding with these residues. Also, in the case of adenosine, its 5′-OH group formed a H-bond with Ser277 (7.42). The NH-group of the ethylcarboxamide moiety of **4**, which is important for the activation of ARs,[21] was found at a distance of 4.5 Å from the OH-group of Thr88 (3.36). Both Ser277 (7.42) and Thr88 (3.36) were previously proposed with the site-directed mutagenesis being critical for agonist but not for antagonist activity (Supporting Information).

The orientation of side chains in proximity to the ligand obtained after InducedFit docking of NECA was compared with their orientation in the A_{2A} AR crystal structure. The superimposition of all non-H atoms of amino acid residues located within 4 Å around **4** in the model obtained and the correspond-

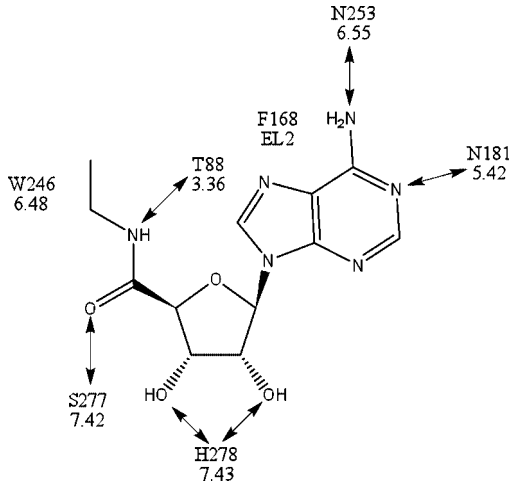

Figure 5. General binding mode of the ARs agonists (**4** shown as a prototypical agonist) proposed on the basis of the molecular modeling and site-directed mutagenesis data. The putative H-bonds are shown by arrows. See to ref 11 for a review of the basis for these predicted interactions. Mutation of the hydrophilic residues proposed to coordinate the ribose moiety (Thr88, Ser277, and His278) has been shown to affect agonist binding selectively.

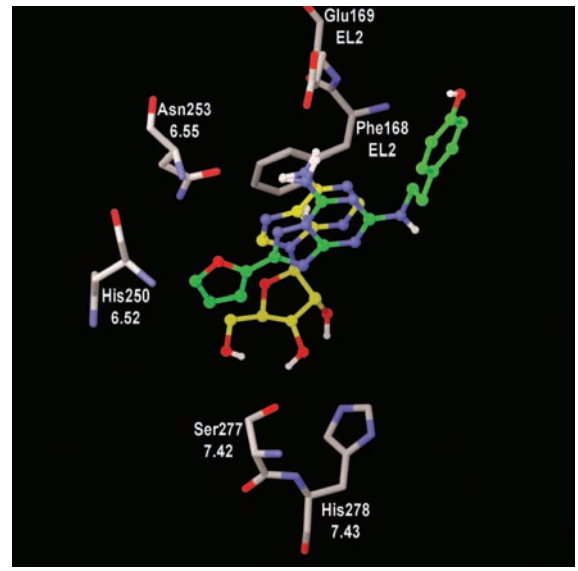

Figure 6. Superimposition of a computationally docked agonist adenosine (yellow) and co-crystallized antagonist **1** (green) inside the binding site of the crystal structure of the A_{2A} AR.

ing atoms of the receptor crystal structure provided an rmsd value of 0.65 Å. The side chains of most of the residues were found in their original conformations. However, the terminal amido group of Asn253 (6.55) was rotated by 68°, and the carboxylic group of Glu169 (EL2) was rotated by 67°. In addition, the side chain of Met270 (7.35) was shifted by 2.9 Å, and the indole ring of Trp246 (6.48) shifted approximately by 1 Å outward from **4**.

Figure 5 shows the general binding mode of the ARs agonists proposed previously based on molecular modeling and site-directed mutagenesis data. Thus, the binding mode obtained after the docking of adenosine and **4** to the experimental structure of the A_{2A} AR is almost identical to their binding mode proposed in previous modeling studies and remains in good agreement with the mutagenesis data.

The previous studies of the binding modes of AR ligands suggested that the agonist adenine ring and an antagonist aromatic system should be accommodated in the same region within the putative binding site of the receptor.[10] Our present results of molecular docking of adenosine and **4** have fully confirmed that hypothesis. The overlay of adenosine and **1** inside the A_{2A} AR is shown in Figure 6. The adenine moiety of adenosine and the triazolotriazine fragment of **1** have very similar positions inside the binding site and are involved in similar interactions with the receptor, namely, with Phe168 (EL2), Glu169 (EL2), and Asn253 (6.55). In agreement with previous molecular modeling studies of ARs, the A_{2A} AR agonists were found to be located between TMs 3, 5, 6, and 7. Moreover, in a comparison of corresponding atoms of the two docked structures both the ring N atoms and the exocyclic amines are in proximity to each other. The adenine C2-position of the agonists was oriented toward the extracellular part of the receptor. Therefore, C2 side chains of functionalized A_{2A} AR agonists[22] could occupy the same region as the phenylethylamino chain of **1**. Previously, it was predicted with molecular modeling that the 2-hydroxypropenyl moiety of 2-hydroxypropenyl-substituted derivatives of adenosine or **4** can interact with residues located in the second extracellular loop (EL2), namely, with Cys166.[7] Similarly, the phenylethylamine chain of **1** in the X-ray structure is also oriented toward the ELs. Thus, the orientation and contact points of the modeled agonist adenine ring inside the receptor were almost identical to those of the bicyclic triazolotriazine core of **1**.

Discussion

The crystallographic structure of the A_{2A} AR was reasonably approximated using rhodopsin-based molecular modeling. Several key features of this receptor structure previously identified through the combination of modeling and mutagenesis were validated in the X-ray study.[6,16] Overall, residues of the upper half of TMs 3, 5, 6, and 7 and of EL2 were predicted to be involved in ligand recognition, and this was the case in the X-ray structure. The crystallographic structure also revealed the direct involvement of EL2 in coordination of **1**. The role of the ELs in ligand recognition has been well supported by modeling and mutagenesis.[24,25] Thus, in cases where an X-ray structure is lacking, the homology modeled structure of a given family A GPCR could be considered a reasonable template for further modeling, with the possible exception of the extracellular and intracellular loops.

Molecular docking of **1** to its native binding site of the A_{2A} AR crystal structure performed with different methods and different constraints resulted in different binding modes predicted. We found that the most accurate position of the ligand can be obtained by molecular docking performed in the presence of water molecules as they appeared in the ligand binding site of the crystal structure. However, if the receptor structure is unknown, the prediction of the position of the water molecules inside the binding site is problematic. Using the ligand−receptor interactions proposed based on the site-directed mutagenesis data can also significantly improve the accuracy of molecular docking. Our results demonstrated that the experimental binding mode of **1** can be reproduced using only one constraint, namely, the H-bond between the exocyclic amino group of the ligand and the side chain oxygen atom of Asn253 (6.55). Thus, our results demonstrated that the molecular docking approach can be successfully applied to accurately reproduce an experimentally observed binding mode of a GPCR ligand. On the other hand, these data revealed the difficulties in the prediction of a ligand binding mode if the experimental data are limited. In addition and not surprisingly, even if the crystal structure of a receptor is available, the results of molecular docking are

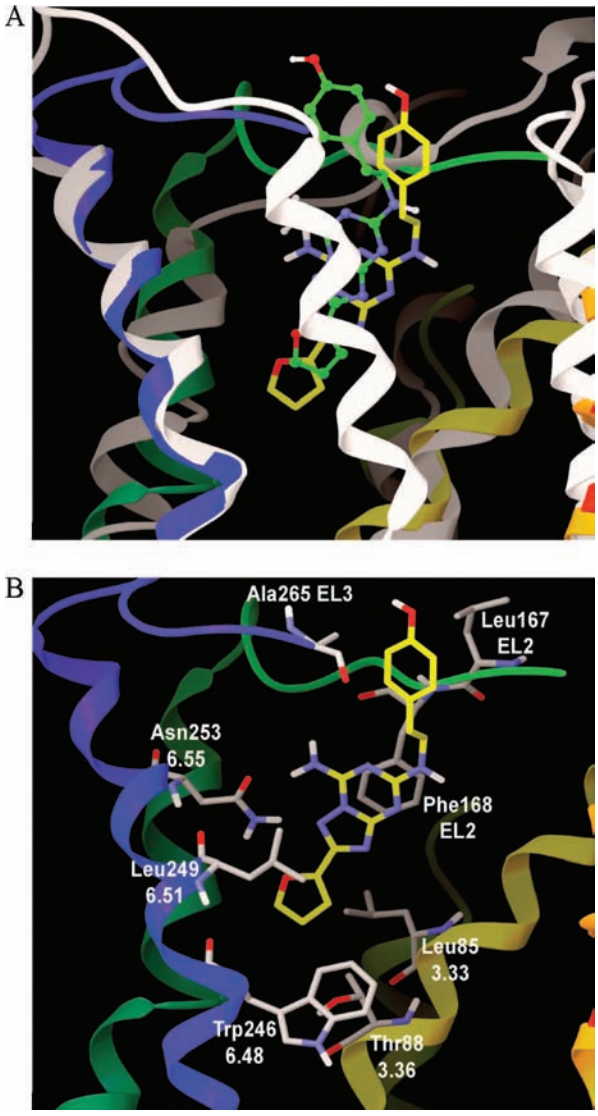

Figure 7. (A) Superimposition of the model (TMs are colored, ligand C-atoms in yellow) and crystal (TMs in white, ligand C-atoms in green) structure of the A_{2A} AR complexed with the antagonist **1**. (B) Binding mode of **1** obtained after molecular docking to the homology model of the A_{2A} AR. The main ligand−receptor interactions observed in the model are similar to interactions appearing in the crystal structure.

extremely dependent on the software and protocols used for the molecular docking. These might also be the reasons for differences between the binding mode of **1** as appearing in the crystal structure and previously predicted binding modes of analogous AR antagonists.

The recently published X-ray structure of the A_{2A} AR did not predict a docking mode for agonists. Therefore, a molecular modeling approach is still relevant, as it has been utilized in our recent drug design and receptor reengineering efforts that focused mainly on agonists. The fact that the agonist affinity of the T4-lysozyme construct of the A_{2A} AR used in the X-ray study is even enhanced over the WT receptor[4] would seem to justify this approach.

Several molecular models of ARs with their various agonists have been published; for a detailed review, see Costanzi et al.[12] On the basis of the predictions made with modeling combined with experimental data of site-directed mutagenesis, we proposed a typical binding mode for ARs agonists, shown in Figure 4 for adenosine and the potent, nonselective agonist **4**. It was suggested that the N^6-amino group of the adenine ring of adenosine derivatives most likely forms a H-bond with Asn253 (6.55).[6,26] Another hydrophilic residue, Asn181 (5.42), was predicted to be involved in H-bonding with the adenine ring N1-nitrogen atom. The ligand ribose ring was predicted to lie within a predominantly hydrophilic region. The 2′- and 3′-groups of the ribose ring were predicted to be located in proximity to His278 (7.43), which is conserved among the ARs. Experimental data indicate that the conserved His residue (7.43) is involved in H-bonding with the OH-groups of the ligand ribose ring. This proximity was indicated in a study of neoceptors, in which the ligand was modified in a fashion complementary to the single amino acid mutation of an AR.[17,27,28] In the proposed molecular models, Ser277 (7.42) and Thr88 (3.36) were involved in H-bonding with the 5′-OH group of adenosine derivatives and with the ethylcarboxamide moiety of analogues of **4**. Mutation of Thr88 in A_{2A} AR neoceptors suggests a proximity to the terminal position of the 5′-uronamide.[26] It was concluded that the ribose-binding region is the most important for receptor activation.

It is noted that the ligand−receptor interactions mentioned above were observed for two different conformations with respect to the glycosidic bond of adenosine and its derivatives. Molecular docking of various adenosine analogues to the rhodopsin-based models of all four ARs demonstrated the preferences for an anti-conformation of the glycosidic bond.[7,37−39] However, computational studies of activation of the A_{2A} AR performed by Kim and co-workers indicated the preferences of an intermediate conformation in the model obtained after rotation of the highly conserved Trp246 (6.48).[6] In the present study, both agonists, adenosine and **4**, docked in the crystallographic structure of the A_{2A} AR adopted an anti-conformation.

Docked agonist ligands display a close correspondence between the orientation of the adenine moiety and the heterocyclic moiety of the antagonist **1** in the crystallographic structure. Several sources of evidence support this mode of overlay of the agonist nucleobase and triazolotriazine moieties, including parallel SAR (structure−activity relationship) between agonist and antagonist series.[9,29,30] Also, the exocyclic amino group common to both chemical classes has been suggested to form a H-bond with Asn253. The importance of this critical residue for both agonist and antagonist binding has been supported with mutagenesis.

The overlay of AR agonists and antagonists has long been a concern in light of the structural similarities of nucleobase and core heterocycles of the antagonists. Three older hypotheses treated the mode of overlay of purine agonists and purine (e.g., xanthine) antagonists.[31] In particular, it is possible to superimpose N1, N3, N7, and N9 nitrogen atoms of the purine ring of adenosine with the corresponding nitrogen atoms of theophylline. However, in this case the positive electrostatic potential of the exocyclic amino group of adenosine corresponds to the negative electrostatic potential of the carbonyl oxygen atom of theophylline. In view of this, van Galen et al. suggested the overlap of N1, N3, N7, and N9 atoms of the adenine ring with the C2, C6, N9, and N7 atoms, respectively, of the xanthine moiety.[32] Since the binding of N^6-substituted adenosine derivatives correlates well with the binding of C8-substituted xanthines it was proposed that substituents at these positions can occupy the same place inside the receptor.[29] The superimposition of the N1, N3, N9 atoms of the adenine ring with the N9, N3, and N1 atoms of xanthine ring was suggested.[33] Since we have not studied xanthine binding to the A_{2A} AR in this study, we cannot distinguish these possibilities. However, our present study predicts that the correspondence model in which N is mapped

on N applies to antagonists such as **1**, in which there is an exocyclic NH. This correspondence of amino groups was previously used to develop A_3 selective antagonists through acylation of the amino group in the heterocyclic series.[36] Other parallels in SAR with nucleoside agonists, i.e., at the 2 position, have been found in the series of adenine antagonists, which also have an exocyclic NH.[34]

The inaccuracy and uncertainty of the modeling approach applies more to the docking to the A_{2A} AR rather than its protein structural prediction, at least in the TM region. This problem is somewhat alleviated if there is a likely anchor point, such as an electrostatic bridge for the biogenic amine and nucleotide (P2Y) receptors.[2,25] Moreover, the prediction of the correct binding mode of an antagonist seems to be a more difficult goal than modeling of the agonist-bound receptor. Small molecule agonists of a given family A GPCR are perhaps more likely than antagonists to occupy a conserved region of the receptor because of a commonality in the receptor activation mechanism.[35] In theory, in order to block agonist action, antagonists need to overlap with the docked position of agonists only partially. Thus, the hypothesis that antagonists display a more diverse range of docking modes than agonists is reasonable. Although the orientation of the **1** antagonist in the X-ray structure was shifted toward the extracellular region in comparison to the previously obtained orientation of a distantly related antagonist **2**, many of the same amino acid residues predicted in the modeling are involved. Some receptor antagonists, such as the secondary propanolamines of the β_2AR and the truncated nucleosides of the A_3 AR,[21] are more likely to occupy the same binding mode as agonists because of structural similarity. Thus, in comparison to **1** the position of carazolol in the β_2 adrenergic receptor is closer to the position of retinal in rhodopsin and, as predicted here, the position of adenosine in the A_{2A} AR. Finally, in this modeling study we have predicted that the key heterocyclic pharmacophore of the antagonist **1** closely overlays the purine moiety of adenosine agonists.

The problem of flexibility of the loops has been discussed in the literature, and in general, differences in configuration between the computational models and the experimental structure were expected. For this reason, in some models of GPCRs the extracellular and intracellular loops were not constructed at all. The EL2 of the A_{2A} AR crystallographic structure is more similar to the β-adrenergic receptors than to rhodopsin. Not surprisingly, it was possible to obtain a similar docked mode of **1** using as a template the β_2 adrenergic receptor crystallographic structure, which has a more extended EL2 structure. Basing the previous models of ARs on rhodopsin possibly introduced some distortion of the docked ligand structure due to steric crowding in the region of EL2. This distortion of the homology model is particularly relevant to ligands such as **1**, which have an extended chain. The presence of chains in functionalized congeners of both AR agonist and antagonist ligands anticipated that part of these extended ligands would protrude into the extracellular region.[29] Also, Duong et al.[30] demonstrated that mutagenesis of a charged residue in EL2 of another AR subtype, the A_3 AR, selectively increased affinity in C2 derivatives of adenosine, in which a long chain was modified in a complementary fashion. The C2 substituent of adenosine agonists would correspond to the 2-phenylethylamino chain of **1**, according to our agonist docking hypothesis.

To summarize, a comparison of the recently published crystal structure of the A_{2A} AR and its structure predicted with the molecular modeling revealed similarities not only in the general configuration of TMs but also in the position and orientation of side chains of amino acid residues involved in ligand recognition. Analysis of the ligand−receptor interactions observed in the X-ray structure fully confirmed much of the previous data obtained with rhodopsin-based homology modeling and site-directed mutagenesis. Molecular docking of AR agonists to the A_{2A} AR crystal structure provided a similar agonist binding mode to that previously predicted on the basis of the A_{2A} AR homology models. The utilization of the β_2AR-based model of the A_{2A} AR receptor for the docking of **1** provided an accurate approximation of the experimentally observed binding mode of this A_{2A} AR antagonist. Thus, our findings have demonstrated that homology modeling of GPCRs remains a useful technique in probing the structure of the protein and predicting modes of ligand docking. Further insights in ligand binding will be gained from crystallization of the ARs with chemically diverse ligands, including adenine derivatives.

Methods

Homology Modeling. The MOE software was utilized to construct a homology model of the human A_{2A} AR. The recent crystal structure of the β_2AR was used as a template. The sequence alignment of the A_{2A} AR and β_2AR was performed with the MOE program taking into account positions of residues highly conserved for all GPCRs. Only a part (Cys166−Asn175) of EL2 was modeled. A total of 25 independent models were built, and the highest scoring intermediate model was chosen automatically as the final model. The geometry optimization was performed with the AMBER99 force field. The Reaction Field salvation model was used. The "Fine" option was selected for both intermediate and final models refinement. The energy minimization of intermediate models was terminated when the root mean square (rms) of the energy gradient fell below 1.0; for the final model the value of the rms gradient was set to 0.5 $kcal \cdot mol^{-1} \cdot Å^{-1}$.

Molecular Docking of A_{2A} AR Agonists. The InducedFit docking procedure of the Schrödinger Macromodel package was utilized to dock adenosine and **4** to the X-ray structure of the A_{2A} AR. The receptor grid generation was performed for a box with the center in the centroid of **1**. The box size was determined automatically. The default values of 0.50 were used for the receptor and ligand van der Waals scaling during initial Glide docking. The number of poses to remain after initial docking was set to 30. The residues located within 5.0 Å of the docked ligand were subjected to refinement with the Prime. The optimization of side chains was enabled. The structures within 30.0 $kcal \cdot mol^{-1}$ of the best structure were redocked.

Molecular Docking of Antagonist 1 to the A_{2A} AR Crystal Structure. The A_{2A} AR crystal structure was used for molecular docking of 1. Three different approaches were used: Schrodinger Glide XP, InducedFit, and MOE Tabu Search docking. In all cases the size of the docking box was determined automatically. The center of the docking box had a center in the centorind of **1** inside the crystal structure of the A_{2A} AR in its experimental position and conformation. For all, Glide XP, InducedFit docking, and MOE-dock, their default parameters were used.

Molecular Docking of Antagonist 1 to the β_2AR-Based Model. The β_2AR-based model of the A_{2A} AR was used for molecular docking of **1**. The automatic docking was performed with the MOE-dock tool implemented in MOE software. A 3D docking box with a side of 24 Å was defined with the center placed in the centroid of Thr88, Phe168, Asn181, Trp246, His250, Asn253, Ser277, and His278. The standard parameters of the Tabu Search (1000 steps/run, 10 attempts/step, 10 Tabu list length) protocol were applied. The default value of 25 docking runs was used. The calculations were performed in the MMFF94x force field.

To refine the orientation of the receptor side chains, the complex of the A_{2A} AR with **1** docked was subjected to the MCMM calculations. The MCMM calculations were performed with the

Schrödinger Macromodel software. **1** and all amino acid residues located within 4 Å from the ligand were subjected to the MCMM search. A shell of constrained residues located within an additional 2 Å from **1** was used. The maximum number of steps was set to 100, and the energy window for saving structures was set to 100.0 $kJ \cdot mol^{-1}$. Water was used as an implicit solvent. A maximum of 500 interactions of Polak−Ribier conjugate gradient (PRCG) minimization method with a convergence threshold of 0.05 $kJ \cdot mol^{-1} \cdot Å^{-1}$ was used.

Acknowledgment. This research was supported by the Intramural Research Program of the NIH, National Institute of Diabetes and Digestive and Kidney Diseases. We thank Dr. Stefano Costanzi (NIDDK) and Dr. Soo-Kyung Kim (California Institute of Technology) for helpful discussions.

Supporting Information Available: Table of mutational analysis of selected residues of the human A_{2A} AR and relation to the predicted agonist binding interactions. This material is available free of charge via the Internet at http://pubs.acs.org.

References

(1) (a) Palczewski, K.; Kumasaka, T.; Hori, T.; Behnke, C. A.; Motoshima, H.; Fox, B. A.; Le Trong, I.; Teller, D. C.; Okada, T.; Stenkamp, T. E.; Yamamoto, M.; Miyano, M. Crystal structure of rhodopsin: a G protein-coupled receptor. *Science* **2000**, *289*, 739–745. (b) Okada, T.; Sugihara, M.; Bondar, A.-N.; Elstner, M.; Entel, P.; Buss, V. The retinal conformation and its environment in rhodopsin in light of new 2.2 Å crystal structure. *J. Mol. Biol.* **2004**, *342*, 571–583.

(2) Rusmussen, S. G. F.; Choi, H.-J.; Rosenbaum, D. M.; Kobilka, T. S.; Thian, F. S.; Edwards, P. C.; Burghummer, M.; Ratnala, V. R. P.; Sanishvili, R.; Fischetti, R. F.; Schertler, G. F. X.; Weis, W. I.; Kobilka, B. K. Crystal structure of the human β_2-adrenergic G-protein-coupled receptor. *Nature (London)* **2007**, *450*, 383–388.

(3) Warne, T.; Serrano-Vega, M. J.; Baker, J. G.; Moukhamedzianov, R.; Edwards, P. C.; Henderson, R.; Leslie, A. G. W.; Tate, C. G.; Schertler, G. F. X. Structure of a β_1-adrenergic G-protein-coupled receptor. *Nature (London)* **2008**, *454*, 486–492.

(4) Jaakola, V.-P.; Griffith, M. T.; Hanson, M. A.; Cherezov, V.; Chien, E. Y. T.; Lane, J. R.; IJzerman, A. P.; Stevens, R. C. The 2.6 angstrom crystal structure of a human A_{2A} adenosine receptor bound to an antagonist. *Science* **2008**, *322*, 1211–1217.

(5) Kim, J.; Wess, J.; van Rhee, M.; Schöneberg, T.; Jacobson, K. A. Site-directed mutagenesis identifies residues involved in ligand recognition in the human A_{2A} adenosine receptor. *J. Biol. Chem.* **1995**, *270*, 13987–13997.

(6) Kim, S.-K.; Gao, Z.-G.; Van Rompaey, P.; Gross, A. S.; Chen, A.; Van Calenbergh, S.; Jacobson, K. A. Modeling the adenosine receptors: comparison of the binding domains of A_{2A} agonists and antagonists. *J. Med. Chem.* **2003**, *46*, 4847–4859.

(7) Ivanov, A. A.; Palyulin, V. A.; Zefirov, N. S. Computer aided comparative analysis of the binding modes of the adenosine receptor agonists for all known subtypes of adenosine receptors. *J. Mol. Graphics Modell.* **2007**, *25*, 740–754.

(8) Michielan, L.; Bacilieri, M.; Schiesaro, A.; Bolcato, C.; Pastorin, G.; Spalluto, G.; Cacciari, B.; Klotz, K. N.; Kaseda, C.; Moro, S. Linear and non-linear 3D-QSAR approaches in tandem with ligand-based homology modeling as a computational strategy to depict pyrazolo-triazolo-pyrimidine antagonists binding site of the human adenosine A_{2A} receptor. *J. Chem. Inf. Model.* **2008**, *48*, 350–363.

(9) Jacobson, K. A.; Gao, Z.-G. Adenosine receptors as therapeutic targets. *Nat. Rev. Drug Discovery* **2006**, *5*, 247–264.

(10) Poucher, S. M.; Keddie, J. R.; Singh, P.; Stoggall, S. M.; Caulkett, P. W.; Jones, G.; Collis, M. G. The in vitro pharmacology of ZM 241385, a potent, non-xanthine A2a selective adenosine receptor antagonist. *Br. J. Pharmacol.* **1995**, *115*, 1096–1102.

(11) Costanzi, S. On the applicability of GPCR homology models to computer-aided drug discovery: a comparison between in sililco and crystal structures of the β_2-adrenergic receptor. *J. Med. Chem.* **2008**, *51*, 2907–2914.

(12) Costanzi, S.; Ivanov, A. A.; Tikhonova, I. G.; Jacobson, K. A. Structure and function of G protein-coupled receptors studied using sequence analysis molecular modeling and receptor engineering: adenosine receptors. *Front. Drug Des. Discovery* **2007**, *3*, 63–79.

(13) Cristalli, G.; Lambertucci, C.; Marucci, G.; Volpini, R.; Dal Ben, D. A_{2A} adenosine receptor and its modulators: overview on a druggable GPCR and on structure−activity relationship analysis and binding requirements of agonists and antagonists. *Curr. Pharm. Des.* **2008**, *14*, 1525–1552.

(14) Ballesteros, J.; Weinstein, H. Integrated methods for the construction of three-dimensional models of structure−function relations in G protein-coupled receptors. *Methods Neurosci.* **1995**, *25*, 366–428.

(15) Lei, S.; Javitch, J. A. The binding site of aminergic G protein-coupled receptors: the transmembrane segments and second extracellular loop. *Annu. Rev. Pharmacol. Toxicol.* **2002**, *42*, 437–467.

(16) IJzerman, A. P.; Von Frijtag Drabbe Künzel, J. K.; Kim, J.; Jiang, Q.; Jacobson, K. A. Site-directed mutagenesis of the human adenosine A_{2A} receptor. Critical involvement of Glu13 in agonist recognition. *Eur. J. Pharmacol.* **1996**, *310*, 269–272.

(17) Jacobson, K. A.; Gao, Z. G.; Chen, A.; Barak, D.; Kim, S. A.; Lee, K.; Link, A.; Van Rompaey, P.; Van Calenbergh, S.; Liang, B. T. Neoceptor concept based on molecular complementarity in GPCRs: a mutant adenosine A_3 receptor with selectively enhanced affinity for amine-modified nucleosides. *J. Med. Chem.* **2001**, *44*, 4125–4136.

(18) *Molecular Operating Environment*, version 2009.05; Chemical Computing Group: Montreal, Canada.

(19) Mohamadi, F. N.; Richards, G. J.; Guida, W. C.; Liskamp, R.; Lipton, M.; Caufield, C.; Chang, G.; Hendrickson, T.; Still, W. C. MacroModel, an integrated software system for modeling organic and bioorganic molecules using molecular mechanics. *J. Comput. Chem.* **1990**, *11*, 440–467.

(20) Sherman, W.; Day, T.; Jacobson, M. P.; Friesner, R. A.; Farid, R. Novel procedure for modeling ligand/receptor induced fit effects. *J. Med. Chem.* **2006**, *49*, 534–553.

(21) Melman, A.; Wang, B.; Joshi, B. V.; Gao, Z. G.; de Castro, S.; Heller, C. L.; Kim, S. K.; Jeong, L. S.; Jacobson, K. A. Selective A_3 adenosine receptor antagonists derived from nucleosides containing a bicyclo-[3.1.0]hexane ring system. *Bioorg. Med. Chem.* **2008**, *16*, 8546–8556.

(22) Barrington, W. W.; Jacobson, K. A.; Hutchison, A. J.; Williams, M.; Stiles, G. L. Identification of the A_2 adenosine receptor binding subunit by photoaffinity crosslinking. *Proc. Natl. Acad. Sci. U.S.A.* **1989**, *86*, 6572–6576.

(23) Yuzlenko, O.; Kieć-Kononowicz, K. Molecular modeling of A_1 and A_{2A} adenosine receptors: comparison of rhodopsin and β_2-adrenergic-based homology models through the docking studies. *J. Comput. Chem.* **2009**, *30*, 14–32.

(24) Kim, J.; Jiang, Q.; Glashofer, M.; Yehle, S.; Wess, J.; Jacobson, K. A. Glutamate residues in the second extracellular loop of the human A_{2a} adenosine receptor are required for ligand recognition. *Mol. Pharmacol.* **1996**, *49*, 683–691.

(25) Moro, S.; Hoffmann, C.; Jacobson, K. A. Role of the extracellular loops of G protein-coupled receptors in ligand recognition: a molecular modeling study of the human $P2Y_1$ receptor. *Biochemistry* **1999**, *38*, 3498–3507.

(26) Jacobson, K. A.; Ohno, M.; Duong, H. T.; Kim, S. K.; Tchilibon, S.; Cesnek, M.; Holy, A.; Gao, Z. G. A neoceptor approach to unraveling microscopic interactions between the human A_{2A} adenosine receptor and its agonists. *Chem. Biol.* **2005**, *12*, 237–247.

(27) Jiang, Q.; Lee, B. X.; Glashofer, M.; van Rhee, A. M.; Jacobson, K. A. Mutagenesis reveals structure−function parallels between human A_{2A}-adenosine receptors and the biogenic amine family. *J. Med. Chem.* **1997**, *40*, 2588–2595.

(28) Jiang, Q.; van Rhee, M.; Kim, J.; Yehle, S.; Wess, J.; Jacobson, K. A. Hydrophilic side chains in the third and seventh transmembrane helical domains of human A_{2A} adenosine receptors are required for ligand recognition. *Mol. Pharmacol.* **1996**, *50*, 512–521.

(29) Jacobson, K. A.; Kirk, K. L.; Padgett, W.; Daly, J. W. Probing the adenosine receptor with adenosine and xanthine biotin conjugates. *FEBS Lett.* **1985**, *184*, 30–35.

(30) Duong, H. T.; Gao, Z. G.; Jacobson, K. A. Nucleoside modification and concerted mutagenesis of the human A_3 adenosine receptor to probe interactions between the 2-position of adenosine analogs and Gln167 in the second extracellular loop. *Nucleosides, Nucleotides Nucleic Acids* **2005**, *24*, 1507–1517.

(31) Dudley, M. W.; Peet, N. P.; Demeter, D. A.; Weintraub, H. J. R.; IJzerman, A. P.; Nordvall, G.; van Galen, P. J. M.; Jacobson, K. A. Adenosine A1 receptor and ligand molecular modeling. *Drug. Dev. Res.* **1993**, *28*, 237–243.

(32) van Galen, P. J. M.; van Vlijmen, H. W. T.; IJzerman, A. P.; Soudjin, W. A model for the antagonist binding site on the adenosine A2 receptor, based on steric, electrostatic, and hydrophobic properties. *J. Med. Chem.* **1990**, *33*, 1708–1713.

(33) Peet, N. P.; Lentz, N. L.; Meng, E. C.; Dudley, M. W.; Ogden, A. M. L.; Demeter, D. A.; Weintraub, H. J. R.; Bey, P. A novel synthesis of xanthines: support for a new binding mode for xanthines with respect to adenosine at adenosine receptors. *J. Med. Chem.* **1990**, *33*, 3127–3130.

(34) Camaioni, E.; Costanzi, S.; Vittori, S.; Volpini, R.; Klotz, K. N.; Cristalli, G. New substituted 9-alkylpurines as adenosine receptor ligands. *Bioorg. Med. Chem.* **1998**, *6*, 523–533.

(35) Wess, J.; Han, S.-J.; Kim, S. K.; Jacobson, K. A.; Li, J. H. Conformational changes involved in G protein-coupled receptor activation. *Trends Pharmacol. Sci.* **2008**, *29*, 616–625.
(36) Baraldi, P. G.; Tabrizi, M. A.; Gessi, S.; Borea, P. A. Adenosine receptor antagonists: translating medicinal chemistry and pharmacology into clinical utility. *Chem. Rev.* **2008**, *108*, 238−263.
(37) Tchilibon, S.; Kim, S. K.; Gao, Z. G.; Harris, B. A.; Blaustein, J. B.; Gross, A. S.; Duong, H. T.; Melman, N.; Jacobson, K. A. Exploring distal regions of the A_3 adenosine receptor binding site: sterically constrained N^6-(2-phenylethyl)adenosine derivatives as potent ligands. *Bioorg. Med. Chem.* **2004**, *12*, 2021–2034.
(38) Ivanov, A. A.; Wang, B.; Klutz, A. M.; Chen, V. L.; Gao, Z. G.; Jacobson, K. A. Probing distal regions of the A_{2B} adenosine receptor by quantitative structure−activity relationship modeling of known and novel agonists. *J. Med. Chem.* **2008**, *51*, 2088–2099.
(39) Palaniappan, K. K.; Gao, Z. G.; Ivanov, A. A.; Greaves, R.; Adachi, H.; Besada, P.; Kim, H. O.; Kim, A. Y.; Choe, S. A.; Jeong, L. S.; Jacobson, K. A. Probing the binding site of the A_1 adenosine receptor reengineered for orthogonal recognition by tailored nucleosides. *Biochemistry* **2007**, *46*, 7437–7448.

JM801533X